

# MHD Flow of Water Base Nano Fluid over a Permeable Stretching Surface with Chemical Reaction

M. Kumari

*L.B.S.Mahavidyalaya, Tilak Nagar Jaipur- 302004, India*

Pratiti Tiwari

*Maharani Gayatri Devi Girls' School Sawai Ram Singh Road, Near Ajmeri Gate, Jaipur-302017, India*

**Abstract**—In the present study, we have investigated MHD flow of water base nanofluid over a permeable surface in the presence of radiation and inclined magnetic field. We have considered Ag-water nanofluid,  $Al_2O_3$ -water nanofluid and Cu- water nanofluid. The governing PDEs have been changed into higher order coupled ODEs and solved numerically by R-K fourth order method with shooting technique. We have discussed the effect of various physical parameters such as Ag-water nano fluid,  $Al_2O_3$ -water nanofluid and Cu- water nanofluid, magnetic parameter (M), Eckert number (Ec), radiation parameter (R) and suction/injection parameter (S) on velocity, temperature and mass profile have been analyzed and depicted graphically. It is noted that on an increase the value of (M) parameter, Alumina-water nanofluid will have higher influence than other nanofluid.

**Index Terms**—Radiation; suction/injection; water base Nanofluid.

## I. INTRODUCTION

The flow of nanofluids over stretching surface have received much importance due to its wide industrial and engineering applications such as drawing of filaments through quiescent fluids, stretching of plastic films, glass fiber production nanofluids as vehicular brake fluids, systems cooling, heating buildings and reducing pollution, space and defense, friction reduction, mass transfer enhancement, industrial cooling applications, solar absorption, energy storage, magnetic sealing, magnetic fluids, biomedical application, friction reduction, nanofluids-based microbial fuel cell, antibacterial activity, etc. In view of these applications Soomro et al. [1] has studied heat transfer analysis of prandtl liquid nanofluid in the presence of homogenous-heterogenous reactions. One of the nice research on nanofluid flow over stretching sheet is carried out by Khan and Pop [2]. Sohail et al. [3] have investigated the radiative slip flow on MHD nanofluid over a stretching sheet. Irfan [4] has investigated a study about MHD water based nanofluid flow over a stretching sheet.

They have also examined effects of thermo-physical effects of water driven copper nanoparticles. Rajotia et al. [5] has investigated viscous dissipation effects in water driven carbon nanotubes. Daniel et al. [6] has proposed slip effects on electrical unsteady MHD natural convection flow of Nanofluid over a permeable shrinking sheet with thermal radiation. The effects of heat and mass transfer on MHD Maxwell nanofluids was presented by Bai et al. [7]. Kashif, Azis et al. [8] have studied convective heat transfer in the boundary layer flow of a Maxwell fluid over a flat plate in the presence of pressure gradient.

The study of MHD effects has applications in various equipments such as MHD generator, pumps, bearing etc. Many researchers have been studied in view of these applications. Chauhan and Agrawal [9] have studied MHD flow and heat transfer in a channel bounded by a shrinking sheet and a porous medium bed. Ibrahim [10] has proposed the effect of induced magnetic field and convective boundary condition on MHD stagnation point flow and heat transfer of upper-convected Maxwell fluid in the presence of nanoparticle past a stretching sheet. Jain and Choudhary [11] has proposed the effects of MHD on boundary layer flow in porous medium due to exponentially shrinking sheet with slip. Jain and Parmar [12] have investigated MHD Maxwell fluid flow through a permeable channel.

Radiation occurs in polymer processing, design of heat exchangers, food-stuff processing, metal extrusion, materials handling, conveyors, production of plastic and rubber, chemical processing equipment in glass fiber. Jain and Choudhary [13] elaborated the Soret and Dufour effects on MHD fluid flow due to moving permeable cylinder with radiation. Parmar [14] has explored unsteady convective boundary layer flow for MHD Williamson fluid over an inclined porous stretching sheet with non-linear radiation. Jain and Bohra [15] studied radiation effects of nano fluid flow through a squeezing rotating channel. Sheikholeslami et al. [16] have

addressed radiation effects on heat transfer on three dimensional nanofluid flow considering thermal interfacial resistance and micro-mixing in suspensions. Nagasasikala and Lavanya [17] have discussed the effects of dissipation and radiation on heat transfer flow of a convective cuo-water nanofluid in a vertical channel. Krishan et al. [18] has studied MHD boundary layer flow of a nanofluid over an exponentially permeable stretching sheet with radiation and heat sourance/sink. Reddy et al. [19] have proposed chemically reacting Maxwell fluid flow post a linear stretching sheet.

Chemical engineering industries and metallurgy, such as food processing and polymer production are some important examples of heat and mass transfer study on fluids with chemical reaction effects. Ojjela and kumar [20] have investigated chemically reacting micropolar fluid flow and heat transfer between expanding or contracting boundary. Shehzad et al. [21] have considered the effects of mass transfer on MHD flow of Casson fluid with chemical reaction and suction. Second law analysis of hydromagnetic couple stress fluid embedded in a non-Darcian porous medium was studied by Opanuga et al. [22]. It has been widely studied by Hayat [23-24], Salem and EI-Aziz [25], Bhattacharyya and Layek [26].

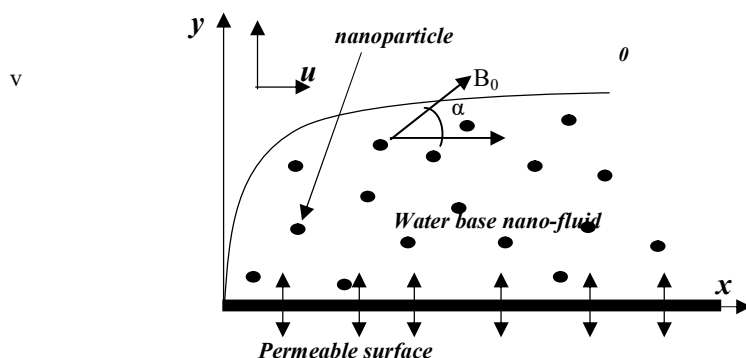


Fig.1 Schematic Diagram the Fluid Flow

In the present paper, we have discussed the heat and mass transfer analysis of inclined MHD water base nanofluids flow over a permeable surface with radiation and chemical reaction. The governing boundary layer equations have been simplified by using suitable similarity transformations. The resulting equations have solved using Runge-Kutta fourth order with shooting technique using MATLAB. The effect of Prandtl number, chemical reaction parameter, radiation parameter, magnetic parameter, Schmit number and suction/injection parameter on the velocity, temperature and concentration profiles have been obtained and presented graphocally. Skinfriction, wall temperature gradient and concentration gradient have been tabulated.

### 1. Mathematical Formulation

We considered a two-dimensional steady flow of an incompressible inclined MHD water base nano fluids over a permeable stretching surface with radiation. The surface is stretched along x-axis with a velocity  $ax$ , where  $a > 0$  is stretching parameter. The fluid velocity, Temperature and nanoparticle concentration near surface are assumed to be  $u_w$ ,  $T_w$  and  $C_w$ , respectively, as shown in Fig. 1. Temperature in the free-stream condition is  $T_\infty$ . For the present problem, the basic equations of conservation of mass, momentum, energy and concentration for a steady flow of nanofluid can be written as:

$$\frac{\partial u}{\partial x} + \frac{\partial v}{\partial y} = 0 \quad (1)$$

$$u \frac{\partial u}{\partial x} + v \frac{\partial u}{\partial y} = \left( \frac{\nu_f}{(1-\phi)^{2.5} (1-\phi + \phi \frac{\rho_s}{\rho_f})} \right) \frac{\partial^2 u}{\partial y^2} - \frac{\sigma B_0^2 u}{\rho_{nf}} \sin^2 \alpha \quad (2)$$

$$u \frac{\partial T}{\partial x} + v \frac{\partial T}{\partial y} = \frac{k_f}{(\rho C_p)_f} \left[ \frac{k_s + (n-1)k_f - 2\phi_1(k_f - k_s)}{(k_s + (n-1)k_f - 2\phi_1(k_f - k_s)) \left( 1 - \phi_1 + \phi_1 \frac{(\rho C_p)_s}{(\rho C_p)_f} \right)} \right] \frac{\partial^2 T}{\partial y^2}$$

$$- \frac{1}{\rho C_p} \frac{\partial q_r}{\partial y} + \frac{\sigma B_0^2}{\rho C_p} u^2 \sin^2 \alpha$$

(3)

$$u \frac{\partial C}{\partial x} + v \frac{\partial C}{\partial y} = D_m \frac{\partial^2 C}{\partial y^2} - k_n (C - C_\infty) \quad (4)$$

subject to boundary conditions

$$y = 0; \quad u = u_w, v = -v_w, T = T_w, C = C_w \quad (5)$$

$$y \rightarrow \infty; \quad u \rightarrow 0, T \rightarrow T_\infty, C \rightarrow C_\infty,$$

where,  $u(x, y)$  and  $v(x, y)$  are the horizontal velocity component and vertical velocity component respectively,  $\rho_f$ ; density of nanofluid,  $\nu_f$ ; kinematic viscosity of nanofluid,  $(\rho C_p)_f$ ; heat capacities of nanofluid, and  $\rho_s$ ; density of nano particles,  $\nu_s$ ; kinematic viscosity of nano particles,  $(\rho C_p)_s$ ; heat capacities of nano particles,  $T$ ; temperature and  $T_\infty$ ; ambient fluid temperature and the surface is stretching with velocity  $u_w = ax$  and  $v_w$  suction/injection velocity.

$$\rho_{nf} = (1 - \phi_1)\rho_f + \phi_1\rho_s, (\rho C_p)_{nf} = (1 - \phi_1)(\rho C_p)_f + \phi_1(\rho C_p)_s,$$

$$\frac{k_{nf}}{k_f} = \left( \frac{k_s + (n-1)k_f - \phi_1(n-1)(k_f - k_s)}{k_s + (n-1)k_f + \phi_1(k_f - k_s)} \right), \mu_{nf} = \frac{\mu_f}{(1 - \phi_1)^{2.5}},$$

where  $n$  is the nanoparticle shape,  $n=3/2$  for cylindrical-shaped nanoparticle and  $n=3$  for spherical-shaped nanoparticles;  $\phi_1$  is the volume fraction of the nanoparticle. Following Rosseland approximation  $q_r$ , the radiation heat flux is given  $q_r = -\left(\frac{4\sigma}{3k^*}\right) \frac{\partial T^4}{\partial y}$ , expanding  $T^4$ , in a Taylor series about  $T_\infty$ , on neglecting higher order term, we get

$$T^4 \approx T_\infty^4 + 4T_\infty^3 T - 4T_\infty^2 T^2 + \dots$$

$$\frac{\partial q_r}{\partial y} = \frac{\partial}{\partial y} \left( \frac{-4\sigma}{3k^*} \frac{\partial T^4}{\partial y} \right) = \frac{\partial}{\partial y} \left( \frac{-4\sigma}{3k^*} \frac{\partial (T_\infty^4 + 4T_\infty^3 T - 4T_\infty^2 T^2)}{\partial y} \right) = \frac{-16\sigma T_\infty^3}{3k^*} \frac{\partial^2 T}{\partial y^2}$$

Governing equation (3) can be written as

$$u \frac{\partial T}{\partial x} + v \frac{\partial T}{\partial y} = \frac{k_f}{(\rho C_p)_f} \left[ \frac{k_s + (n-1)k_f - 2\phi_1(k_f - k_s)}{(k_s + (n-1)k_f - 2\phi_1(k_f - k_s)) \left( 1 - \phi_1 + \phi_1 \frac{(\rho C_p)_s}{(\rho C_p)_f} \right)} \right] \frac{\partial^2 T}{\partial y^2}$$

$$+ \frac{16\sigma T_\infty^3}{3(\rho C_p)_{nf} k^*} \frac{\partial^2 T}{\partial y^2} + \frac{\sigma B_0^2}{(\rho C_p)_{nf}} u^2 \quad (6)$$

## 2. Solution

We now introduce the following relations for  $u, v$  as

$$u = bxf'(\eta), \quad v = -\sqrt{bv_f} f(\eta), \quad \eta = y \sqrt{\frac{b}{v_f}} \quad \theta(\eta) = \frac{T - T_\infty}{T_w - T_\infty}, \quad \phi(\eta) = \frac{C - C_\infty}{C_w - C_\infty} \quad (7)$$

equations (2), (4), (5) and (6) thus reduces to the following non-dimensional form

$$\left( \frac{1}{(1-\phi)^{2.5} \left(1-\phi+\phi \frac{\rho_s}{\rho_f}\right)} \right) f'''' - \frac{Mf'}{\left(1-\phi+\phi \frac{\rho_s}{\rho_f}\right)} \sin^2 \alpha - f'^2 + f'' f = 0 \quad (8)$$

$$\theta'' \left[ \frac{k_s + (n-1)k_f - 2\phi_1(k_f - k_s)}{\left(k_s + (n-1)k_f - 2\phi_1(k_f - k_s)\right) \left(1-\phi_1+\phi_1 \frac{(\rho C_p)_s}{(\rho C_p)_f}\right)} + \frac{4}{3 \left(1-\phi_1+\phi_1 \frac{(\rho C_p)_s}{(\rho C_p)_f}\right)} R \right] + \text{Pr} f \theta' + \frac{\text{Pr} M E c f'^2}{\left(1-\phi_1+\phi_1 \frac{(\rho C_p)_s}{(\rho C_p)_f}\right)} \sin^2 \alpha = 0 \quad (9)$$

$$\phi'' - Sc (K_n \phi - f \phi') = 0 \quad (10)$$

boundary conditions (5) reduces as:

$$\begin{aligned} \eta = 0: & \quad f'(\eta) = \gamma, \quad f(\eta) = S, \quad \theta(\eta) = 1, \phi(\eta) = 1 \\ \eta \rightarrow \infty: & \quad f'(\eta) \rightarrow 0, \quad \theta(\eta) \rightarrow 0, \phi(\eta) \rightarrow 0 \end{aligned} \quad (11)$$

where,  $\text{Pr} = \frac{(\mu C_p)_f}{k_f}$ ; Prandtl number,  $R = \frac{4\sigma T_\infty^3}{kk^*}$ ; radiation parameter,  $k^*$ ; thermal radiation parameter,

$Ec = u_w^2 / C_p (T_w - T_\infty)$ ; Eckert number,  $M = \frac{\sigma B_0^2}{\rho b}$ ; magnetic field parameter,  $\gamma = \frac{a}{b}$ ; shrinking parameter,

$Sc = \frac{\nu_f}{D_m}$ ; Schmidt number,  $K_n = \frac{k_n}{b}$ ; chemical reaction parameter and  $S = \frac{v_w}{\sqrt{v_f b}}$ ; suction/injection parameter.

TABLE I THERMO-PHYSICAL PROPERTIES OF WATER AND NANOPARTICLE

Fluids	$\rho(kg m^{-3})$	$c_p(J kg^{-1} K^{-1})$	$k(Wm^{-1}K^{-1})$
$H_2O$ (Pure Water)	997.1	4179	0.613
Ag (Silver)	10500	235	429
$Al_2O_3$ (Alumina)	3970	765	40
Cu (Copper)	8933	385	400

**TABLE II**

THE SKIN FRICTION COEFFICIENT, LOCAL NUSSELT NUMBER AND LOCAL SHERWOOD NUMBER FOR SILVER WATER BASE NANOFUID

S	M	$\phi$	$\phi$	$\phi$	$f''$	$\theta'$	$\phi'$
-0.5					-1.213489008	-1.195662146	1.008488078
0.0					-1.308256773	-0.713508142	1.578542234
0.5					-1.410429441	0.038734560	2.264258524
	0.0				-1.357748644	2.551464929	2.268435731
	0.5				-1.384355493	1.279834864	2.266319657
	1.0				-1.410429441	0.038734560	2.264258524
		$\phi$			-1.357748644	2.551464929	2.268435731
		$\phi\phi\phi$			-1.410429441	0.038734560	2.264258524
		$\phi\phi\phi$			-1.461093674	-2.359779908	2.260248617
			1.0		-0.532393179	1.208266638	1.886669583
			2.0		-1.410429441	0.038734560	2.264258524
			3.0		-2.523708346	-1.702176512	2.567727930
				0.0	-3.701562119	1.254522656	2.094383218
				0.2	-2.091252986	0.657538739	2.211170425
				0.4	-1.410429441	0.038734560	2.264258524

**TABLE III**

THE SKIN FRICTION COEFFICIENT, LOCAL NUSSELT NUMBER AND LOCAL SHERWOOD NUMBER FOR ALUMINA WATER BASE NANOFUID

S	M	$\phi$	$\phi$	$\phi$	$f''$	$\theta'$	$\phi'$
-0.5					-1.651064085	-0.903493703	0.962406942
0.0					-1.821558597	-0.295411462	1.530032464
0.5					-2.009659704	0.582204096	2.217435914
	0.0				-1.882517247	2.538421183	2.227254870
	0.5				-1.947230866	1.538377964	2.222243920
	1.0				-2.009659704	0.582204096	2.217435914
		$\phi$			-1.882517247	2.538421183	2.227254870
		$\phi\phi\phi$			-2.009659704	0.582204096	2.217435914
		$\phi\phi\phi$			-2.128529945	-1.217681945	2.208317675
			1.0		-0.781721230	1.416744355	1.854324699
			2.0		-2.009659704	0.582204096	2.217435914
			3.0		-3.550011022	-0.743179260	2.510019689
				0.0	-3.701562119	1.254522656	2.094383218
				0.2	-2.690782239	0.949963924	2.166070346
				0.4	-2.009659704	0.582204096	2.217435914

**TABLE IV**  
 THE SKIN FRICTION COEFFICIENT, LOCAL NUSSELT NUMBER AND LOCAL SHERWOOD NUMBER FOR COPPER WATER BASE NANOFLUID

S	M	$\phi$	$\theta$	$\phi$	$f''$	$\theta'$	$\phi'$
-0.5					-1.285876737	-1.076557790	1.000857998
0.0					-1.391921877	-0.552708438	1.570597456
0.5					-1.506715932	0.247506518	2.256645170
	0.0				-1.444320517	2.597414635	2.261575057
	0.5				-1.475871731	1.406394004	2.259075869
	1.0				-1.506715932	0.247506518	2.256645170
		$\phi$			-1.444320517	2.597414635	2.261575057
		$\phi\phi\phi$			-1.506715932	0.247506518	2.256645170
		$\phi\phi\phi$			-1.566455298	-1.983118249	2.251939591
			1.0		-0.571561869	1.309983733	1.881488284
			2.0		-1.506715932	0.247506518	2.256645170
			3.0		-2.690379799	-1.360875888	2.558275582
				0.0	-3.701562119	1.254522656	2.094383218
				0.2	-2.200230215	0.762427330	2.202846247
				0.4	-1.506715932	0.247506518	2.256645170

**TABLE V**  
 THE LOCAL NUSSELT NUMBER AND LOCAL SHERWOOD NUMBER

R	Ec	Kn	Sc	Silver water base nanofluid		Alumina water base nanofluid		Copper water base nanofluid	
				$\theta'$	$\phi'$	$\theta'$	$\phi'$	$\theta'$	$\phi'$
0.0				-0.548020		0.6361564		-0.084174	
0.5				-0.120993		0.6177659		0.1622597	
1.0				0.0387345		0.5822040		0.2475065	
	0.0			2.5469514		2.5277089		2.5920974	
	0.5			1.2928330		1.5549445		1.4197889	
	1.0			0.0387345		0.5822040		0.247506	
		0.0			2.1567725		2.1046232		2.1483301
		0.2			2.2642585		2.2174359		2.2566451
		0.4			2.3666946		2.3242987		2.3597770
			2		2.2642585		2.2174359		2.2566451
			3		3.0037490		2.9583881		2.9963935
			4		3.6886611		3.6446735		3.6815382

TABLE VI

COMPARISON OF  $-f''(0)$  FOR DIFFERENT VALUES Pr IN THE ABSENCE OF THE PARAMETERS  $S = R = K_p = Ec = \phi_1 = 0, \square = 0$

Pr	HAM method Nadeem and Hussain [27]	Gorla and Sidawi [28]	FEM method Goyal and Bhargava [29]	RKF45 method Gorla et al. [34]	K-4 method present study
0.2	0.169	0.1691	0.1691	0.170259788	0.172348764
0.7	0.454	0.5349	0.4539	0.454447258	0.453917857
2	0.911	0.9114	0.9113	0.911352755	0.911361492
7	—	1.8905	1.8954	1.895400395	1.895412536
20	—	3.3539	3.3539	3.353901838	3.353933867

TABLE VII

COMPARISON OF  $-f''(0)$  FOR DIFFERENT VALUES M IN THE ABSENCE OF THE PARAMETERS  $S = R = K_p = \phi_1 = 0, \square \square \square 0$

M	Anderson et al. [30]	Prasad et al. [31]	Mukhopadhyay et al. [32]	Palani et Al. [33]	Present study
0.0	1.000000	1.000174	1.000173	1.00000	1.000000000
0.5	1.224900	1.224753	1.224753	1.224745	1.224744871
1	1.414000	1.414449	1.414450	1.414214	1.414213562
1.5	1.581000	1.581139	1.581140	1.581139	1.581138830
2	1.732000	1.732203	1.732203	1.732051	1.732050808

## II RESULT AND DISCUSSION

Figs. 2–20 represent the velocity, temperature and concentration profiles. Figs. 2-4 exhibit the impacts of suction/injection parameter (S) on momentum, temperature profiles. An increase in the value of S parameter, suppress the velocity, temperature and concentration profile. The effect of suction is to make the velocity and temperature distribution more uniform within the boundary layer. Imposition of fluid suction at the surface has a tendency to reduce both the hydrodynamic and the thermal thickness of the boundary layer. On the other hand, the thermal boundary layer thickness increases with injection which causes a decrease in the rate of heat transfer. Fig. 4 show the impacts of suction/injection parameter (S) on concentration profile. An increase in the suction/injection parameter, decreases the concentration profile. This is due to the fact that suction parameter decelerates fluid particles through porous wall thereby reducing the species boundary layer growth that results in a decrease in the concentration profile. Figs. 5-7 show the influence of M parameter on velocity, heat and concentration profiles. An increase in M parameter suppress the momentum boundary layer thickness and exactly reverse effect have been observed for the temperature and concentration profiles. This is due to the fact that the magnetic field introduces a retarding body force known as Lorentz force. As the Lorentz force is a resistive force which opposes the fluid motion, so heat is produced and as a result, the thermal boundary layer thickness and concentration (volume fraction) boundary layer thickness become thicker for stronger magnetic field. Physically, the drag force increases with an increase in the magnetic field and as a result depreciation occurs in the velocity field.

Figs. 8-10 show the influence of  $\square$  parameter on velocity, temperature and concentration profiles. An increase in  $\square$  parameter suppress the momentum boundary layer thickness and exactly reverse effect have been observed for the heat and concentration profiles. Fig. 11 show the influence of Ec on temperature profile. An Ec, increases the temperature profile also increases. The viscous dissipation produces heat due to drag between the fluid particles and this extra heat causes an increase of the initial fluid temperature. Physically, increasing the values of the Eckert number generates heat in the fluid due to frictional heating. Thus, increasing the values of Ec enhances the temperature within the fluid flow. Fig. 12 show the influences of R on temperature profile. As the R, increase the heat profile also increases. Generally, increasing values of R, the mean absorption coefficient declined, which results in rise to the divergence of radiative heat flux. Hence, the fluid temperature increases as the rate of radiative heat transfer to the fluid shoot up. Figs. 13-15 show the influence of  $\square$  parameters on velocity, heat and concentration profiles. An increase in the  $\square$  parameter rises the momentum boundary layer thickness and temperature gradient whereas exactly reverse effect have been observed for the concentration profiles. The stretching rises pressure on the sheet. Due to this reason we have seen a fall in temperature field and hike in velocity field. Figs. 16-18 show the influence of  $\square$  parameter on velocity, heat and concentration profiles. An increase in the  $\square$  parameters rises the momentum boundary layer thickness and temperature gradient whereas exactly reverse effect have been observed for the concentration profiles. The effect of the Kn and Sc on concentration profile is shown in Figs. 19-20. It is noticed that when value of Kn and Sc parameters are increases then the concentration boundary layer thickness as well as mass profile reduces. Physically, chemical reaction increases the rate of interfacial mass transfer. Chemical reaction suppresses the local

concentration and increases its mass gradient and its flux. It is due to the fact that  $Sc$  is the ratio of velocity to mass diffusivity which means when  $Sc$  increases, mass diffusivity decreases and there is a reduction in mass. Table 2-4 show the effects of some physical parameters on skin friction coefficient, local Nusselt number and local Sherwood number. Table 5 shows the effects on various parameter on local Nusselt number and local Sherwood number. The comparison of the present results with the existed results in ([27], [28], [29], [30], [31], [32], [33], [34]) in Table 6 and 7.

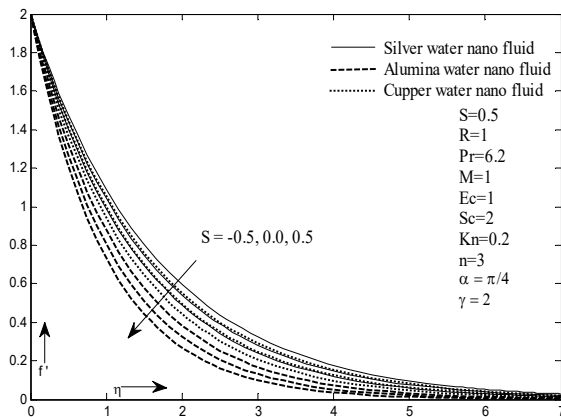


Fig. 2 Influence of S on Momentum profile

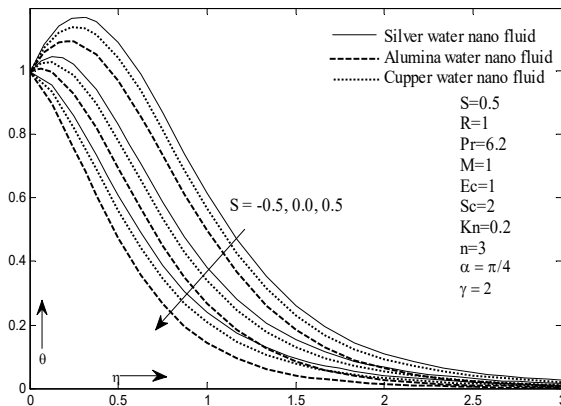


Fig. 3 Influence of S on Temperature profile

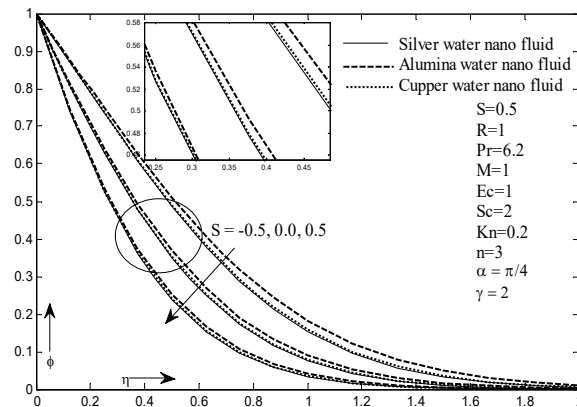


Fig. 4 Influence of S on mass profile



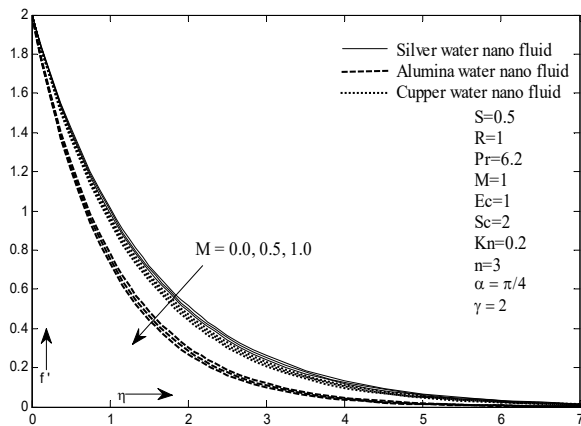


Fig. 5 Influence of M on Momentum profile

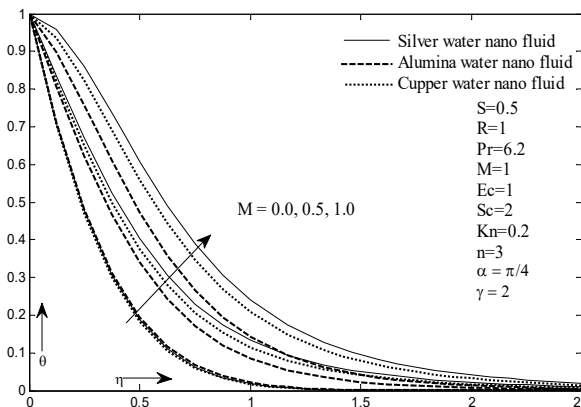


Fig. 6 Influence of M on Temperature profile

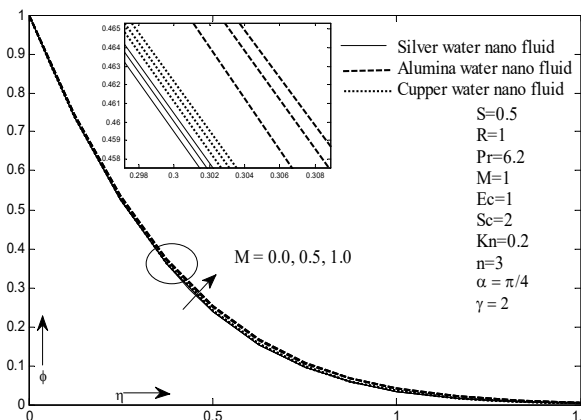


Fig. 7 Influence of M on mass profile

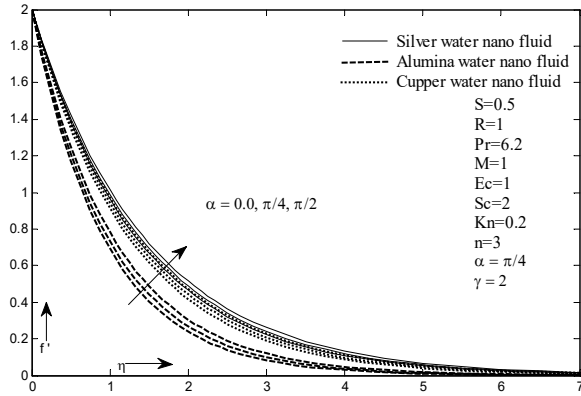


Fig. 8 Influence of  $\alpha$  on Momentum profile

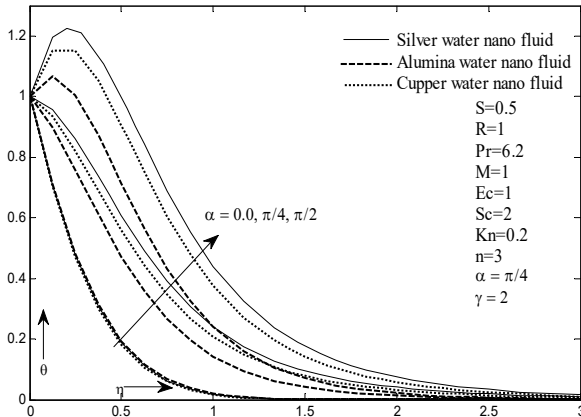


Fig. 9 Influence of  $\alpha$  on Temperature profile

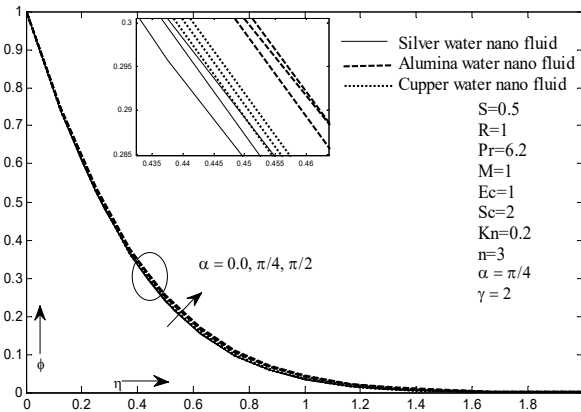


Fig. 10 Influence of  $\alpha$  on mass profile

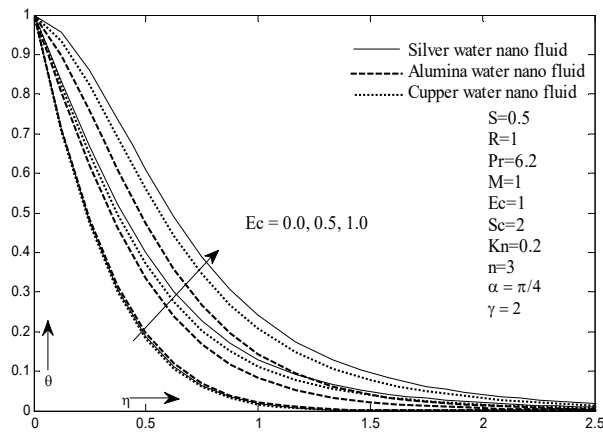


Fig. 11 Influence of  $Ec$  on Temperature profile

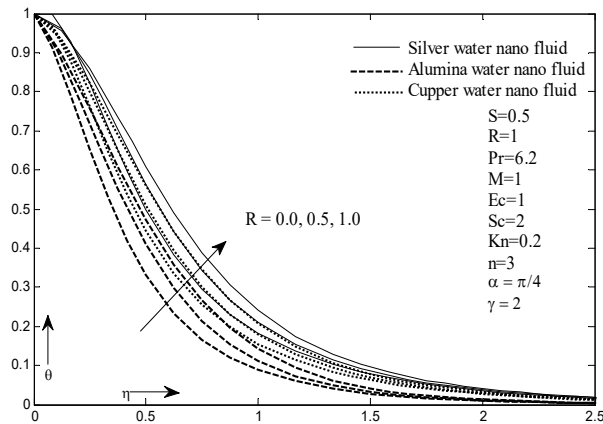


Fig. 12 Influence of  $R$  on Temperature profile

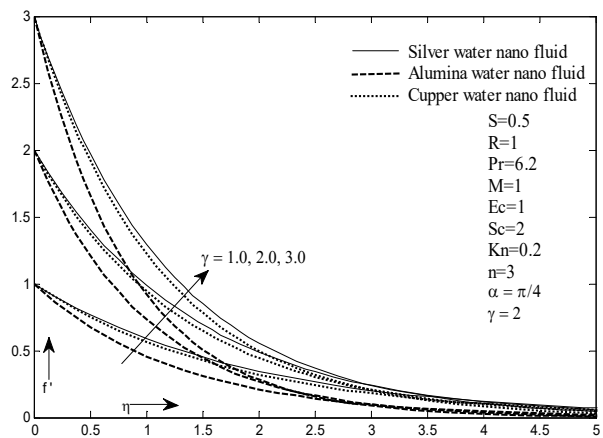


Fig. 13 Influence of  $\gamma$  on Momentum profile

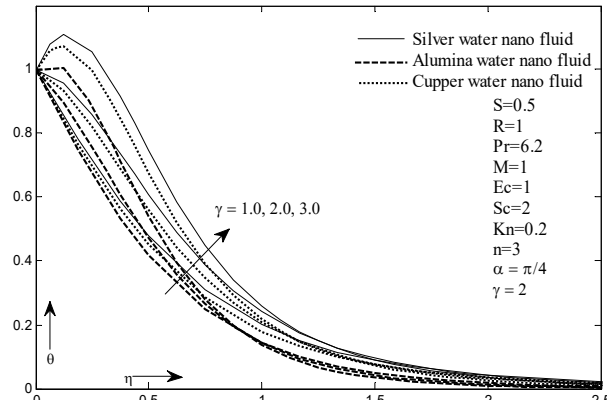


Fig. 14 Influence of  $\gamma$  on Temperature profile

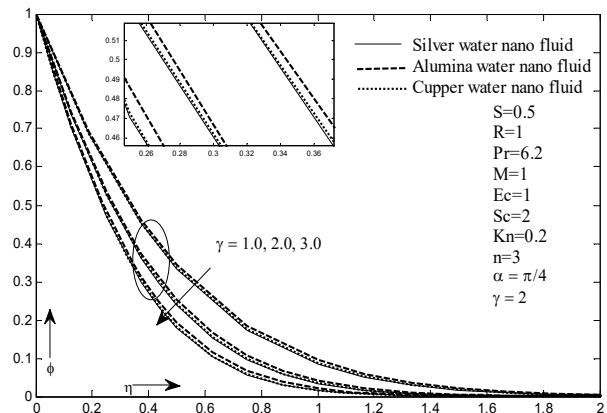


Fig. 15 Influence of  $\gamma$  on mass profile

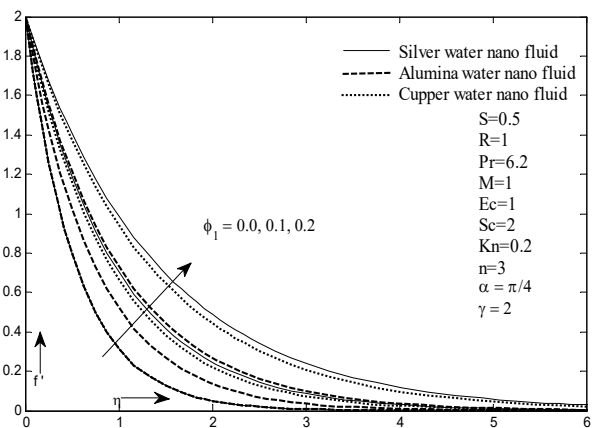


Fig. 16 Influence of  $\phi_1$  on Momentum profile

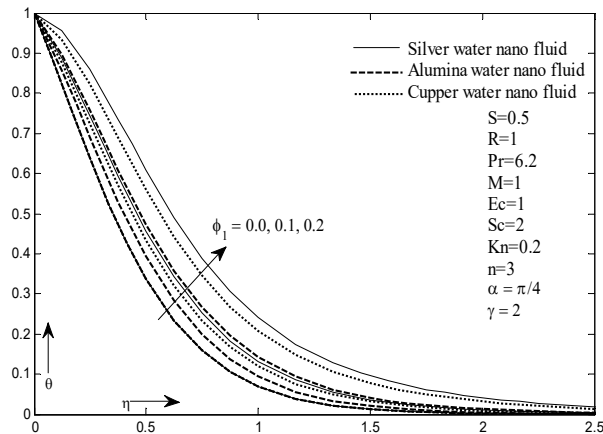


Fig. 17 Influence of  $\phi_1$  on Temperature profile

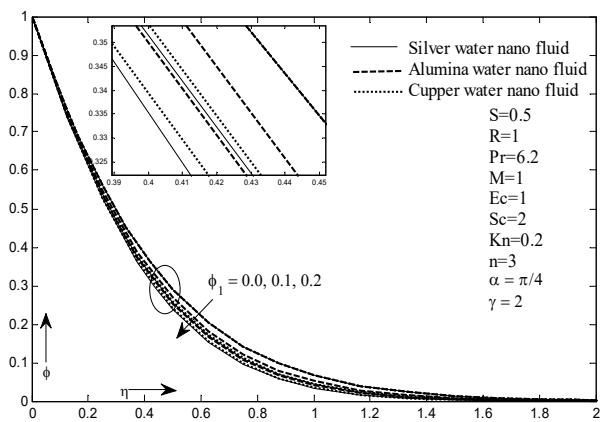


Fig. 18 Influence of  $\phi_1$  on mass profile

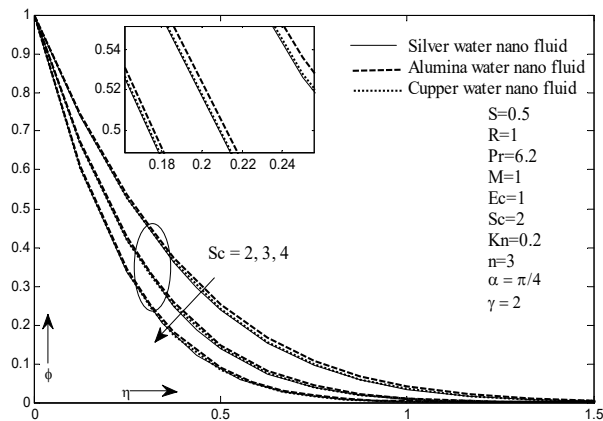


Fig. 19 Influence of  $Sc$  on mass profile

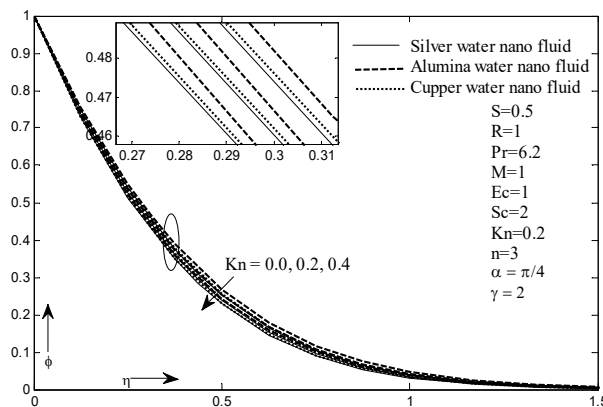


Fig. 20 Influence of Kn on mass profile

### III CONCLUSION

We have investigated MHD flow of water base nanofluid over a permeable stretching surface with chemical reaction. We have considered water base nanofluid such as Ag-water nanofluid and  $Al_2O_3$ -water nanofluid and Cu-water nanofluid.

- It is discerned that heat transfer performance on silver water base nanofluid is better compared to other two fluids on magnetic velocity profile.
- Suction/injection parameter (S) parameter has propensity to suppress the momentum of fluid, thermal heat transfer rate, concentration rate.
- Magnetic field parameter (M) and angle ( $\alpha$ ) has propensity to rise the thermal heat transfer rate and concentration rate whereas inverse impact shows on momentum boundary layer thickness and velocity profile.
- Shrinking parameter ( $\lambda$ ) and the volume fraction of the nanoparticle ( $\phi$ ) parameter has propensity to rise the acceleration of fluid and thermal heat transfer rate whereas inverse impact shows on concentration of fluid.
- Radiation parameter (R) and Eckert number (Ec) has propensity to rise the thermal heat transfer rate of fluid.
- Chemical reaction parameter (Kn) and Schmidt number (Sc) have propensity to suppress the concentration of fluid.
- Rise the value of Schmidt number (S) and coefficient of skin friction oscillates decreases whereas inverse impact shows on rate of heat transfer, rate of mass transfer.
- Rise the value of Magnetic field parameter (M) and coefficient of skin friction oscillates, rate of heat transfer and rate of mass transfer decreases.
- Rise the value of Shrinking parameter ( $\lambda$ ) and coefficient of skin friction oscillates and local Nusselt number decreases whereas inverse impact has been observed on rate of mass transfer.

### IV CONFLICT OF INTERESTS

The authors declare that there is no conflict of interests regarding the publication of this paper.

### REFERENCES

- [1]. F. A. Soomro, R. UIHaq, Z. H. Khan, and Q. Zhang, "Heat transfer analysis of Prandtl liquid nanofluid in the presence of homogenous-heterogeneous reactions", *Results in Phys.*, vol. 10, 2018, pp. 379-384.
- [2]. W. A. Khan, and I. Pop, "Boundary-layer flow of a nanofluid past a stretching sheet", *Int. J. Heat Mass Trans.*, vol. 53, 2010, pp. 2477-83.
- [3]. N. Sohail, H. R. Ul, K. Z. Hayat, and A. N. Sher, "Thermal radiation and slip effects on MHD stagnation-point flow of nanofluid over a stretching sheet", *Phys. E.*, vol. 65, 2015, pp. 17-23.
- [4]. R. Irfan, H. R. Ul, and M. Al-Mdallal Qasem, "Aligned magnetic field effects on water based metallic nanoparticles over a stretching sheet with PST and thermal radiation effects", *Phys. E.*, vol. 89, 2017, pp. 33-42.
- [5]. D. Rajotia, H. R. Ul, and N. F. M. Noor, "Thermo physical effects of water driven copper nanoparticles on MHD axisymmetric permeable shrinking sheet: Dual-nature study", *Eur. Phys. J. E.*, vol. 39, 2016.

- [6]. Y. S. Daniel, Z. A. Aziz, Z. Ismail and F. Salah, "Slip effects on electrical unsteady MHD natural convection flow of Nanofluid over a permeable shrinking sheet with thermal radiation", *Eng. Letters*, 26(1), 2018, pp. 107-116.
- [7]. Y. Bai, X. Liu, Y. Zhang, and M. Zhang, "Stagnation-point heat and mass transfer of MHD Maxwell nanofluids over a stretching surface in the presence of thermophoresis", *J. Mol. Liq.*, vol. 224, 2016, pp. 1172–80.
- [8]. A. N. Kashif, Z. A. Aziz, F. Salah, and K.K. Viswanathan, "Convective heat transfer in the boundary layer flow of a Maxwell fluid over a flat plate using an approximation technique in the presence of pressure gradient", *Eng. Letters*, vol. 26(1), 2018, pp.14-22.
- [9]. D. S. Chauhan, and R. Agrawal, "MHD flow and heat transfer in a channel bounded by a shrinking sheet and a porous medium bed: Homotopy analysis method", *ISRN Thermodyn.*, pp. 1-10, 2013, DOI: 10.1155/2013/291270.
- [10]. W. Ibrahim, "The effect of induced magnetic field and convective boundary condition on MHD stagnation point flow and heat transfer of upper-convected Maxwell fluid in the presence of nanoparticle past a stretching sheet", *Propulsion and Power Research*, vol. 5(2), 2016, pp. 164–175.
- [11]. Jain and Parmar, "Radiative boundary-layer flow of an MHD Maxwell fluid with non – linear chemical reaction and heat source in a permeable channel", *Int. J. of Heat and Tech.*, vol. 36(4), 2018, pp. 1450-1455.
- [12]. S. Jain, and R. Choudhary, "Effects of MHD on boundary layer flow in porous medium due to exponentially shrinking sheet with slip", *Procedia Eng.*, vol. 127, 2015, pp. 1203–1210.
- [13]. S. Jain, and R. Choudhary, "Soret and Dufour effects on MHD fluid flow due to moving permeable cylinder with radiation", *Global and stochastic analys.*, SI: pp. 75-84, 2017.
- [14]. A. Parmar, "Unsteady convective boundary layer flow for MHD Williamson fluid over an inclined porous stretching sheet with non-linear radiation and heat source," *Int. J. of Applied and Comput. Mathe.*, 2017, DOI:10.1007/s40819-017-0373-4.
- [15]. Jain and Bohra, "Hall Current and Radiation Effects on Unsteady MHD Squeezing Nanofluid Flow in a Rotating Channel with Lower Stretching Permeable Wall", *Appl. Of Fluid dyn.*, 2017, pp. 127-141.
- [16]. M. Sheitcholesami, H. R. Kataria, and A. S. Mittal, "Radiation effects on heat transfer on three dimensional nanofluid flow considering thermal interfacial resistance and micro-mixing in suspensions", *Chinese J. of Phy.*, vol. 55, 2017, pp. 2254-2272.
- [17]. M. Nagasasikala, and B. Lavanya, "Effects of dissipation and radiation on heat transfer flow of a convective cuo-water nanofluid in a vertical channel", *J. of Adv. Res. in Fluid Mech. and Thermal Sci.*, vol. 50, 2018, pp. 108-117.
- [18]. N. Krishan, C. Kalyani, and M. C. Reddy, "MHD boundary layer flow of a nanofluid over an exponentially permeable stretching sheet with radiation and heat source/sink", *Trans.phenom. Nano Micro Scales*, vol. 4(1), 2016, pp. 44-51.
- [19]. A. M. Reddy, J. V. R. Reddy, N. Sandeep, and V. Sugunamma, "Chemically reacting Maxwell fluid flow past a linear stretching sheet", *Appl. and Appl. Mathe.*, vol. 12, 2017, pp. 259-274.
- [20]. O. Ojjela, and N. N. kumar, "Chemically reacting micropolar fluid flow and heat transfer between expanding or contracting boundary with ion slip, Soret and Dufour effects," *Alexandria Engg. J.*, vol. 55, 2016, pp. 1683-1694.
- [21]. S. A. Shehzad, T. Hayat, M. Qasim, and S. Asghar, "Effects of mass transfer on MHD flow of Casson fluid with chemical reaction and suction", *Brazilian J. of Che. Eng.*, vol. 30 (1), 2013, pp. 187 – 195.
- [22]. A. A. Opanuga, J. A. Gbadeyan, and S. A. Iyase, "Second Law Analysis of Hydromagnetic Couple Stress Fluid Embedded in a Non-Darcian Porous Medium," *IAENG Int. J. of Appl. Mathe.*, vol. 47(3), 2017, pp. 287-294.
- [23]. T. Hayat, M. I. Khan, M. Waqas, A. Alsaedi, and M. Farooq, "Numerical simulation for melting heat transfer and radiation effects in stagnation point flow of carbon– water nanofluid", *Comput. Methods Appl. Mech. Eng.*, vol. 315, 2017, pp. 1011–24.
- [24]. T. Hayat, M. Waqas, S. A. Shehzad, and A. Alsaedi, "Mixed Convection Stagnation-Point Flow of Powell-Eyring Fluid with Newtonian Heating, Thermal Radiation, and Heat Generation/Absorption", *J. Aerosp. Eng.*, 04016077-8, 2016.
- [25]. A. M. Salem, and M. A. El-Aziz, "Effect of Hall currents and chemical reaction on hydromagnetic flow of a stretching vertical surface with internal heat generation/absorption", *Appl. Mathe. Mode*, vol. 32, 2008, pp. 1236.
- [26]. K. Bhattacharyya, and G. C. Layek, "Slip effect on diffusion of chemically reactive species in boundary layer flow over a vertical stretching sheet with suction or blowing", *Chemical Eng. Commun.*, vol. 198, 2011, pp. 1354.
- [27]. S. Nadeem, and S. T. Hussain, "Flow and heat transfer analysis of Williamson nanofluid", *Appl. Nanosci.*, vol. 4(8), 2013, 1005–1012.
- [28]. R. S. R. Gorla, and I. Sidawi, "Free convection on a vertical stretching surface with suction and blowing", *Appl. Sci. Res.*, vol. 52(3), 1994, 247–257.
- [29]. M. Goyal, and R. Bhargava, "Boundary layer flow and heat transfer of viscoelastic nanofluids past a stretching sheet with partial slip conditions", *Appl. Nanosci.*, vol. 4(6), 2014, pp. 761–767.
- [30]. H. I. Andersson, O. R. Hansen, and B. Holmedal, "Diffusion of a chemically reactive species from a stretching sheet", *Int. J. Heat Mass Trans.*, vol. 37, 1994, pp. 659–64.
- [31]. K. V. Prasad, A. Sujatha, K. Vajravelu, and I. Pop, "MHD flow and heat transfer of a UCM fluid over a stretching surface with variable thermos-physical properties", *Meccanica*, vol. 47, 2012, 1425–39.
- [32]. S. Mukhopadhyay, A. M. Golam, and A. P. Wazed, "Effects of transpiration on unsteady MHD flow of an UCM fluid passing through a stretching surface in the presence of a first order chemical reaction", *Chin Phys B* 22:124701, 2013.
- [33]. S. Palani, B. R. Kumar, and P. K. Kameswaran, "Unsteady MHD flow of an UCM fluid over a stretching surface with higher order chemical reaction", *Ain Shams Eng. J.*, vol. 7, 2016, pp. 399–408.
- [34]. R. S. R. Gorla, B. C. Prasannakumara, B. J. Gireesha, and M. R. Krishnamurthy, "Effects of chemical reaction and nonlinear thermal radiation on Williamson nanofluid slip flow over a stretching sheet embedded in a porous medium", *J. Aerosp. Eng.*, Vol. 29(5), 2016, 04016019.
- [35]. F. Carapau, P. Correia, L. M. Grilo, and Ricardo Conceicao, "Axisymmetric motion of a proposed generalized non-Newtonian fluid model with shear-dependent viscoelastic effects", *IAENG Int. J. of Appl. Mathe.*, vol. 48(4), 2018, pp. 361-370.